HIGH RESOLUTION WIND FIELDS OVER THE BLACK SEA DERIVED FROM ENVISAT ASAR DATA USING AN ADVANCED WIND RETRIEVAL ALGORITHM

Werner Alpers[(1)], Alexis Mouche[(2)], Andrei Yu. Ivanov[(3)], Burghard Brümmer[(4)]

(1) Institute of Oceanography, University of Hamburg, Hamburg, Germany, Email: alpers@ifm.uni-hamburg.de

(2) CLS Radar Applications Division, Brest, France, Email: amouche@cls.fr

(3) P.P. Shirshov Institute of Oceanology, Russian Academy of Sciences, Moscow, Russia, Email: ivanoff@ocean.ru

(4) Meteorological Institute, University of Hamburg, Hamburg, Germany, Email: burghard.bruemmer@zmaw.de

ABSTRACT

Recently a new wind retrieval algorithm has been proposed by Mouche et al. (2012) which uses for wind direction retrieval also the Doppler shifts induced by motions of the sea surface. The extraction of Doppler shifts from synthetic aperture radar (SAR) data requires a special analysis of the complex SAR data. This new wind retrieval algorithm uses all three sources of information on wind direction (atmospheric model, linear features on SAR images, and Doppler shift) and combines them using the Bayesian method. In this investigation we apply this new algorithm for three complex wind events that occurred over the Black Sea and which were captured by the Advanced SAR (ASAR) onboard the Envisat satellite. Because of the complex coastal topography of the Black Sea, which gives rise to various local wind fields, it is an ideal sea area to test algorithms to retrieve sea surface winds from SAR data. It is demonstrated that the new wind retrieval algorithm yields, in general, better results than the conventional algorithms. However, since the measured Doppler shifts contain also contributions from surface currents, care has to be taken to account properly for this correction, which is not always straightforward, as shown in the last wind event analysed in the paper.

1. INTRODUCTION

The Black Sea is a sea area surrounded by mountains of differing heights with valleys opening to the sea. Local winds blowing onto the sea over coastal mountains or through valleys as well as meso-scale atmospheric eddies are often encountered over the Black Sea. Thus it is an ideal area to study complex wind systems and their interaction. The interaction of local winds, like foehn winds, gap winds, katabatic winds, and atmospheric eddies with synoptic-scale winds or with each other give rise to wind fronts in which often rain cells are embedded [1], [2]. Synthetic aperture radar (SAR) provides an ideal means to study fine-scale structures of near-surface wind fields over waters. In contrast to scatterometers, which measure near-surface wind speeds and directions with a spatial resolution of the order of ten kilometres, SARs can measure it with a resolution of the order of 100 m. However, the retrieval of two-dimensional wind fields from SAR data is not as straightforward as from scatterometer data, since SAR cannot measure wind directions directly. While scatterometers measure the backscattered radar power or normalized radar cross section (NRCS) from a resolution cell from (at least) three different azimuth directions, SARs only measure it from one azimuth direction, which is perpendicular to the satellite flight direction. Thus, in order to retrieve (two dimensional) wind fields from SAR images, one has to get the wind direction from other sources than from backscattered radar power values [3]-[6]. In most previous investigations the wind direction was obtained either from 1) atmospheric models or 2) linear features often visible on SAR images of the sea surface. In this investigation we apply a new wind retrieval algorithm, which uses for wind direction retrieval also the Doppler shifts induced by motions of the sea surface by Mouche et al. (2012) [6]. The extraction of Doppler shifts from SAR data requires a special analysis of the complex SAR data. This new wind retrieval algorithm uses all three sources of information on wind direction (atmospheric model, linear features, and Doppler shift) and combines them using the Bayesian method. We apply this new algorithm to three complex wind events with winds blowing from different directions over the Black Sea. The near-surface wind field is retrieved from SAR data which were acquired in 2010 and 2011 by the Advanced SAR (ASAR) on board the Envisat satellite, which operates at C-band (5.3 GHz). It is demonstrated that the new wind retrieval gives better results than the conventional wind retrieval algorithms. The SAR-derived wind data are compared with model winds. The paper is organized as follows: In section 2 we briefly describe the conventional wind retrieval algorithm using the NRCS together with wind directions from a numerical atmospheric model. In section 3 we introduce the Doppler centroid anomaly, and in section 4 we describe how Doppler information is included in the

Proc. of 'SEASAR 2012', Tromsø, Norway
18-22 June 2012 (ESA SP-709, March 2013)

wind retrieval algorithm. In sections 5 to 7 we present three ASAR images acquired over the Black Sea and derive from them near-surface wind fields using first the conventional wind retrieval algorithm and then the one, in which Doppler information is included. Finally, in section 8 we summarize the results and draw conclusions.

2. CONVENTIAL WIND RETRIEVAL

The conventional wind retrieval algorithm presented in this paper uses for the inversion of NRCS values given by the SAR image the C-band Wind Scatterometer Model Function (GMF) version 4 (CMOD4) [7], which was originally developed to retrieve near-surface wind fields from data of the scatterometer onboard the European Remote Sensing Satellites ERS-1 and ERS-2. The ASAR onboard the Envisat satellite has in the Wide Swath Mode (WSM) a resolution of 150 m and a pixel spacing of 75 m. However, for wind speed estimation, the pixels are averaged over 500 m x 500 m.

For the wind direction, we use the wind field provided by the National Centers for Environmental Prediction (NCEP) Global Forecast System (GFS) model. The GFS model developed by NCEP provides global wind fields every 3 hours at a grid spacing of 0.5° in latitude and longitude. Thus the direction in the SAR-derived wind field is only resolved to a resolution of the order of 100 km

3. DOPPLER CENTROID ANOMALY

It has been demonstrated by Chapron et al. (2005) [8], that Doppler centroid anomaly or, in short, Doppler anomaly (DA), of Envisat ASAR data can be used to retrieve geophysical information about both winds and sea surface currents. The DA or residual Doppler results from the line-of-sight motions of the surface scattering elements relative to the fixed earth. Only the component along the SAR look direction is detected. The DA depends on the relative velocities of the wind and currents, as well as on their directions relative to the SAR antenna look direction. DA data obtained from complex Envisat ASAR data has been used to study strong surface currents [9]. But they also can be used to obtain information on wind direction provided that the contributions from surface currents and wind-induced motions are properly separated. An empirical function, called CDOP, which relates the Doppler shift at C-band to surface winds and radar parameters, has been developed:

$$f^{\mathbf{DA}} = \mathrm{CDOP}(\Phi, u^{10}, \theta, \mathrm{pol}).$$

Here u^{10} denotes the wind speed at a height of 10 m, Φ the angle between the look direction of the SAR antenna and the wind direction, θ the incidence angle, and pol the polarization of the radar.

The CDOP function has been obtained from a three-layer neural network analysis by comparing a large number of wind products from the Advanced Scatterometer (ASCAT) onboard the European MetOp satellite collocated with C-band Doppler anomalies from ASAR [10].

DA data are available on a regular basis in Envisat ASAR WSM products as auxiliary data since July 2007. The pixel spacing in azimuth direction is about 8 km. In range direction it varies between 8 km (in near range) and 3.5 km (in far range). The accuracy of the DA is about 5 Hz corresponding to a horizontal surface velocity change of 20 cm/s at an incidence angle of 40°, and of 40 cm/s at an incidence angle of 20° [11].

4. WIND RETRIEVAL INCLUDING DOPPLER INFORMATION

Portabello et al. (2002) [12] first proposed a methodology to combine SAR information with *a priori* information, taking into account that all sources of information (both observations and models) may contain errors. Mouche et al. (2012) [6] have extended this method by adding information contained in the Doppler shift. Simultaneous observations of NRCS (or σ^0) and Doppler shift (f^{DA}) are assumed to be independent and related to the wind vector $\mathbf{u}$ by the CMOD4 and CDOP transfer functions, respectively. Following Portabello et al. 2002 [12], we assume Gaussian errors for observational data, GMFs, and the model. This leads to a minimization problem for the determination of the maximum probability to get a wind vector $\mathbf{u}$ from measured σ^0 and f^{DA} values [6]:

$$J(\mathbf{u}) = \left(\frac{f^{DA} - \mathrm{CDOP}(\mathbf{u})}{\Delta f^{DA}}\right)^2 + \left(\frac{\mathbf{u} - \mathbf{u}_B}{\Delta \mathbf{u}}\right)^2 \Bigg|_{\left\{u_{10} = \mathrm{GMF}^{-1}(\theta, \phi, \sigma^0, \mathrm{pol}), \phi\right\}}.$$

Here $\mathbf{u}_B$ is the *a priori* wind vector given by the atmospheric model, here by the NCEP model, and $\Delta\sigma^0$, $\Delta f^{\mathbf{DA}}$, and $\Delta\mathbf{u}$ are the Gaussian standard deviation errors for the NRCS, the Doppler anomaly (or Doppler shift), and the model wind vector, respectively. GMF^{-1} is the inverse of the empirical geophysical model unction. Errors in CMOD4 or CDOP and the atmospheric model are expected to be spatially correlated, but not accounted for in this inversion scheme.

5. THE WIND EVENT OF 13 SEPTEMBER 2010

Fig. 1 shows an ASAR image, which was acquired over the Black Sea at 0732 UTC (1132 local standard time) on 13 September 2010 during a descending satellite pass in the WSM mode at VV polarization (vertical polarization for transmission and reception)]. Visible are sea surface signatures of an atmospheric cyclonic eddy, marked by “E”, and of a foehn wind, marked by “F”.

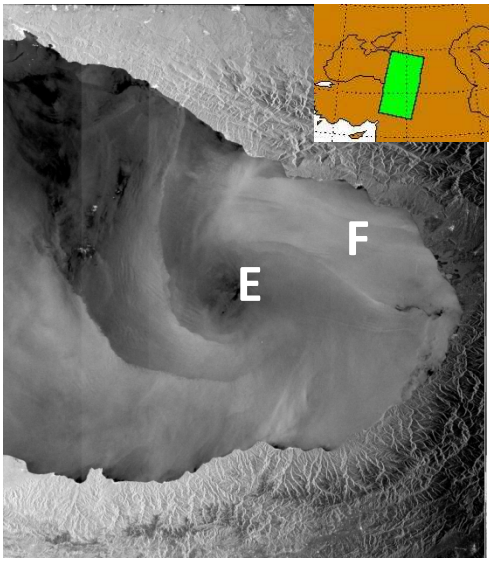

Figure 1. Section of an ASAR image acquired at 0732 UTC on 13 Sep 2010 over the eastern section of the Black Sea showing radar signatures of a mesoscale atmospheric cyclonic eddy (the center marked ‘‘E’’) and a foehn wind (marked ‘‘F’’) . The imaged area is 400 km x 480 km.The inset shows the location of the SAR scene. © ESA

The foehn wind blows through the Kolkhida Lowland (also called Kolkheti Lowland) in the southwestern Caucasus (Western Georgia) onto the sea [1]. The atmospheric eddy results from a positive vorticity advection over the eastern section of the Black Sea as evidenced by the 300-hPa pressure chart valid for 06 UTC on 13 September 2010 (not reproduced here). The atmospheric eddy causes a lifting of air and thus a decrease in air pressure at the sea surface. Thus warm air at low levels spirals into the low pressure center and is forced to rise. As it rises, it cools and forms a spiraling cloud pattern, which is confirmed by the cloud image depicted in Fig. 2. The cloud image depicted in Fig. 2 was acquired by the Moderate Resolution Imaging Spectroradiometer (MODIS) onboard the American Terra satellite at 0830 UTC on 13 September 2010.

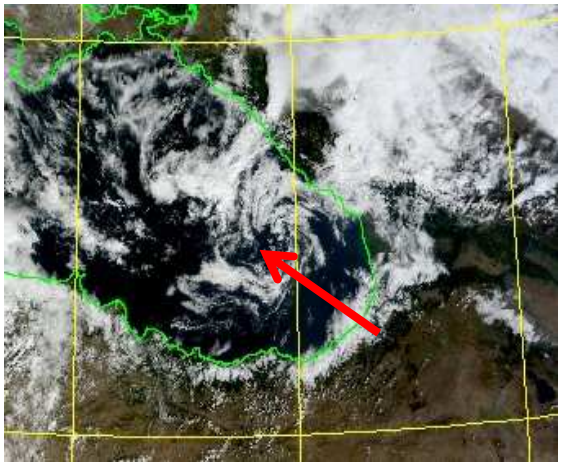

Figure 2. MODIS Terra color composite image acquired at 0830 UTC on 13 September 2010 showing in the eastern section of the Black Sea a cyclonic eddy in the cloud pattern (the red arrow points to its center). The inserted latitude and longitude lines have a grid spacing of 5°. © NASA GSFC

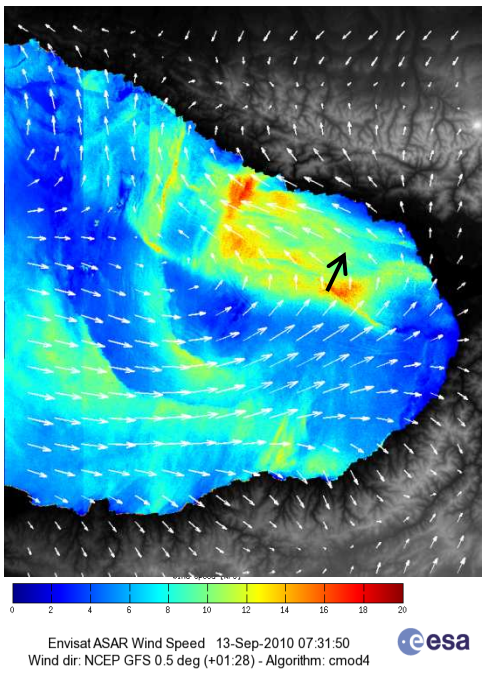

Figure 3. Near-surface wind field derived from the ASAR image depicted in Fig.1 using the wind direction from the NCEP model. Note that in the area of the foehn, wind is blowing into a northeasternly direction (marked by a black arrow), which cannot be correct.

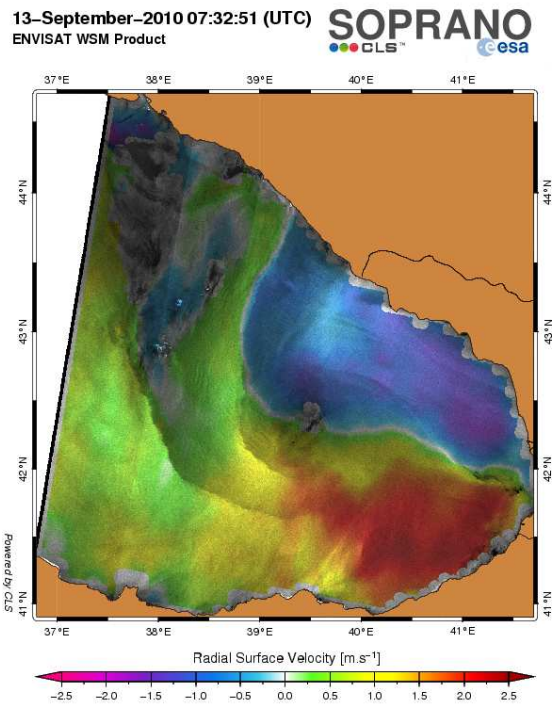

Figure 4. Doppler velocity derived from the ASAR data. Note that in the foehn area the Doppler shift is negative, which implies that the wind is blowing in a westerly direction.

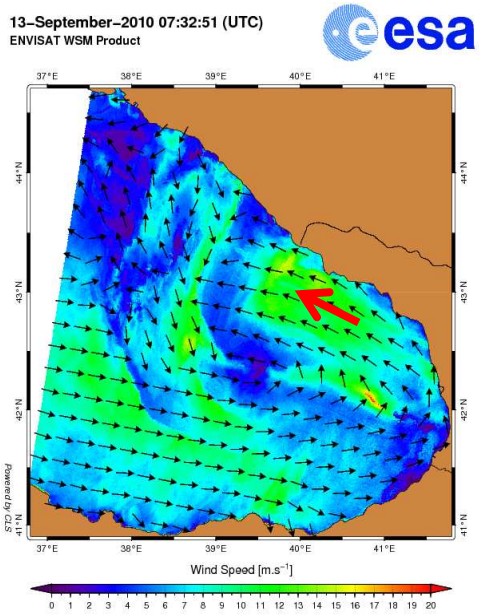

Figure 5. Near-surface wind field derived from the ASAR image depicted in Fig.1 by including Doppler shift information in the wind retrieval algorithm. Now the foehn wind blows in the expected direction, i.e., from land onto the sea (red arrow).

Fig. 4 shows the radial surface velocity inferred from the Doppler shift retrieved from ASAR data. The sign convention is such that negative (positive) radial velocities are velocities directed westward (eastward). In Fig. 3, blue colors denote negative and green/brownish colors positive radial velocities. Thus we infer from the Doppler map that in the foehn area (marked "F" in Fig. 1) the wind was blowing into a westerly direction and that further south, it was blowing in an easterly direction.

When incorporating this Doppler information in the wind retrieval algorithm, we obtain the wind field map depicted in Fig. 5, which shows that now the foehn wind is blowing into the expected direction, i.e., from land (Kolkhida Lowland) onto the sea (red arrow).

6. THE WIND EVENT OF 16 JANUARY 2011

In Fig. 6 another ASAR WSM (VV polarization) image is depicted which shows radar signatures of a complex wind field over the Black Sea. It was acquired at 1919 UTC (2319 local standard time) on 16 January 2011 during an ascending satellite pass (see inset).

On 16/17 January 2011 a cold front was crossing the Black Sea from north to south as evidenced by the surface analysis chart valid for 12 UTC on 16 January (not shown) and the one valid for 00 UTC on 17 January 2011 (Fig. 7). Behind this wind front, a strong wind having speeds between 8 and 12 m/s was blowing in a southwesterly direction as seen on the wind field map depicted in Fig. 8. This wind field map was derived from the ASAR image using the wind direction from the NCEP model valid for 18 UTC on January 2011, which is 1 hour and 19 min earlier than the ASAR data acquisition. Note that on this wind map the wind is blowing into a southeasterly direction on both sides of the front (see red arrows), which is unrealistic. Fig. 9 shows the radial surface velocity inferred from the Doppler shift retrieved from ASAR data. The sign convention is such that positive (negative) radial velocities are velocities directed eastward (westward). When incorporating this Doppler information in the wind retrieval algorithm, we obtain the wind field map depicted in Fig. 10, which shows a quite different wind field than Fig. 8. In particular on this map the wind is now blowing in different directions on both sides of the front (see red arrows).

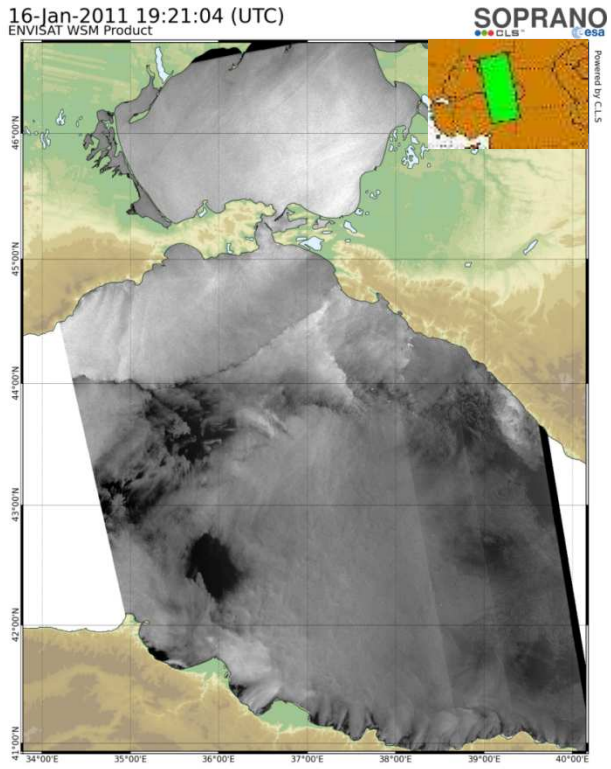

Figure 6. Section of an ASAR WSM (VV polarization) image acquired at 1919 UTC on 16 January 2011 over the eastern section of the Black Sea. The swath width is 400 km. The inset shows the location of the complete SAR scene. © ESA

Figure 7. Section of surface analysis chart valid for 00 UTC on 17 June 2011 showing the passage a cold front over the Black Sea. © UK Met Office.

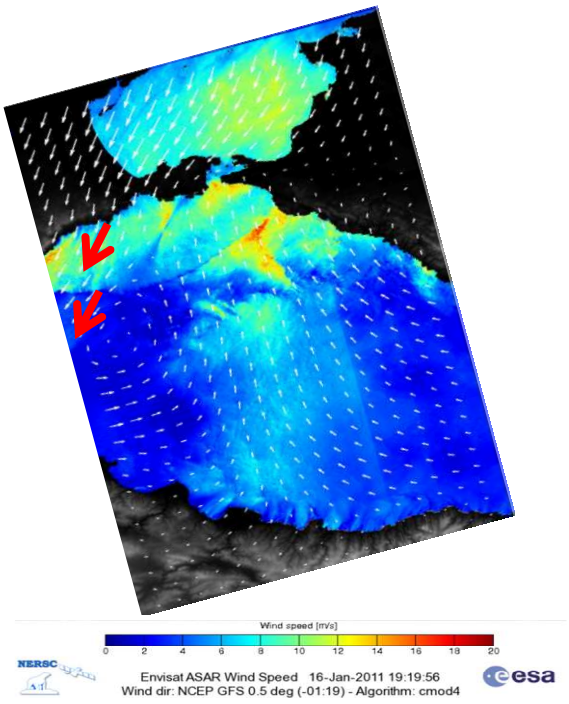

Figure 8. Near-surface wind field derived from the ASAR image depicted in Fig. 6 using the wind direction from the NCEP model. Note that on both sides of the front the wind is blowing in a southeasterly direction (marked by red arrows), which cannot be correct.

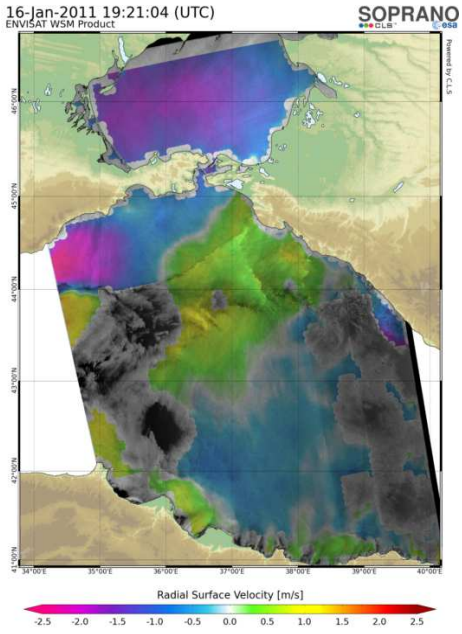

Figure 9. Doppler velocity retrieved from the ASAR data image. Note that on both sides of the front the radial velocities have different signs.

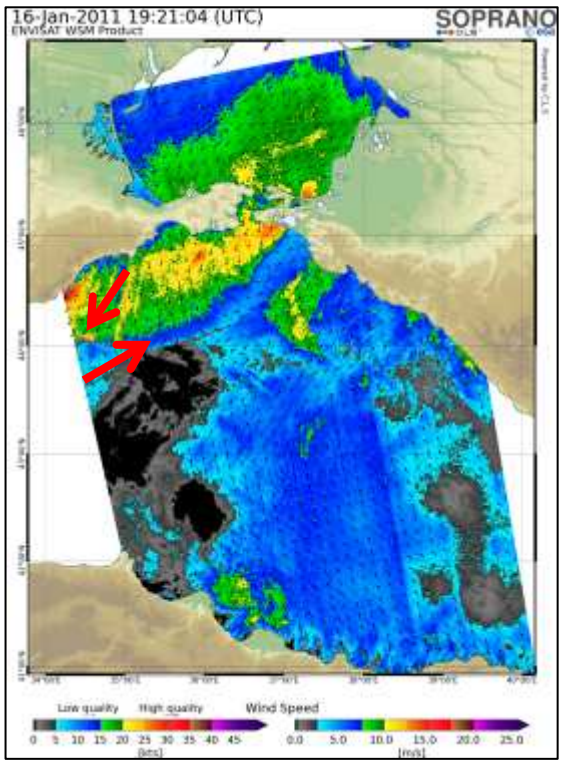

Figure 10. Near-surface wind field derived from the ASAR image depicted in Fig. 6 by including Doppler shift information in the wind retrieval algorithm. Now the wind direction on both sides of the front are different (red arrows)

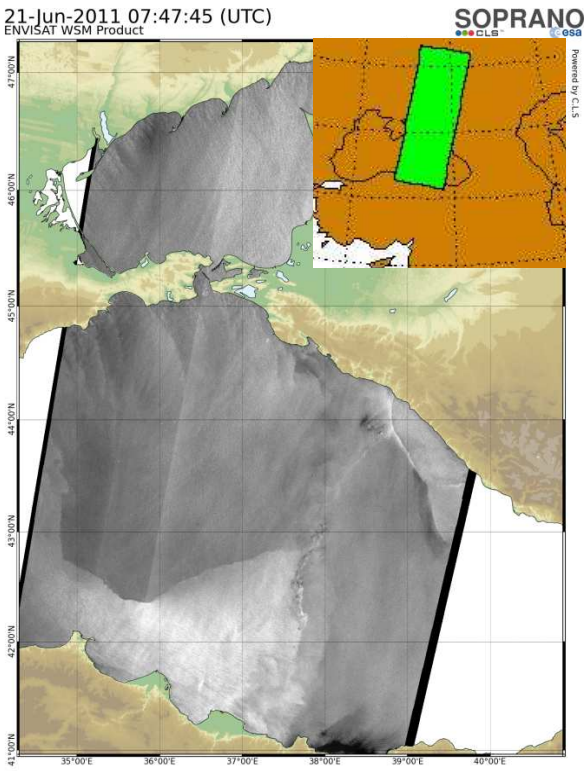

Figure 11. Section of an ASAR WSM image acquired at 0745 UTC on 21 June 2011 over the eastern section of the Black. The swath width is 400 km. The inset shows the location of the complete SAR scene. © ESA

7. THE WIND EVENT OF 21 JUNE 2011

Fig. 11 shows an ASAR WSM (VV polarization) image which was acquired over the Black Sea at 0745 UTC (0932 local standard time) on 21 June 2011 during a descending satellite pass (see inset). Visible is in the southern section a boundary between areas of low and high image intensity, which is caused by the cold front passing the Black Sea (see the surface analysis chart depicted in Fig. 13). As visible on the wind maps depicted in Figs. 14 and 16, this is also the boundary between areas of low and high wind speed. Furthermore, in the central eastern section of the image a bright band (band of high image intensity) attached to the coast is visible. Fig. 12 shows a zoom on this area with the coastal mountains.

From a meteorological point of view one would expect that the wind directions are those marked by the red arrows in Fig. 2. This interpretation is supported by the following observations:

1) The weather station at Tuapse measured at 0600 and 0900 UTC (1000 and 1300 local time) a wind direction from SSE and a wind speed of 5-6 m/s.

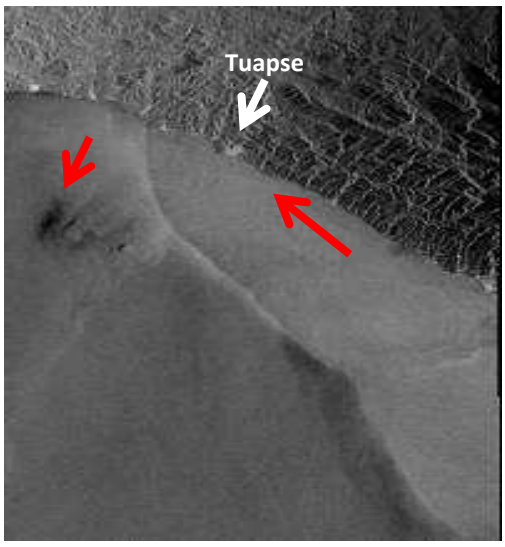

Figure 12. Zoom on the bright band visible on the right on the ASAR image depicted in Fig.11. This section of the ASAR image is presented in the satellite coordinate system and shows also the coastal mountains. The red arrows mark the suspected wind direction.

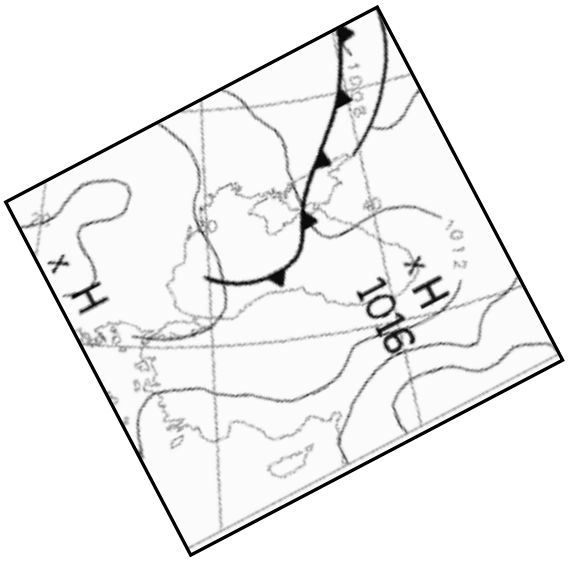

Figure 13. Section of the surface analysis chart valid for 00 UTC on 21 June 2011 showing a cold front over the Black Sea. © UK Met Office.

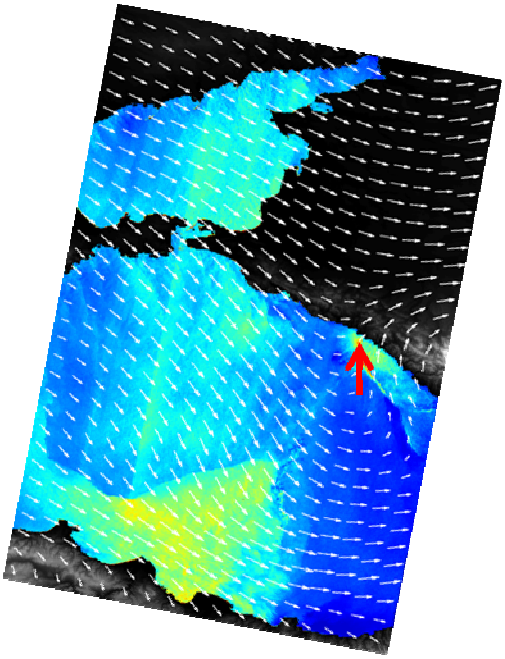

Figure 14. Near-surface wind field derived from the ASAR image depicted in Fig. 11 using the wind direction from the NCEP model. The inserted red arrow shows the wind direction in the area of the wind tongue.

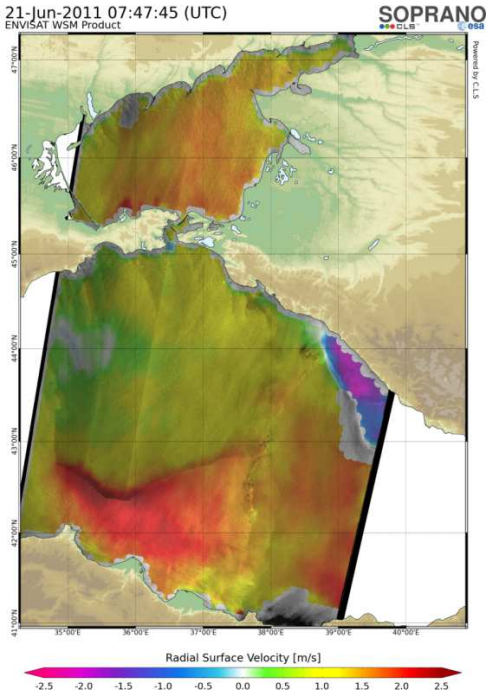

Figure 15. Doppler velocity retrieved from the ASAR data.

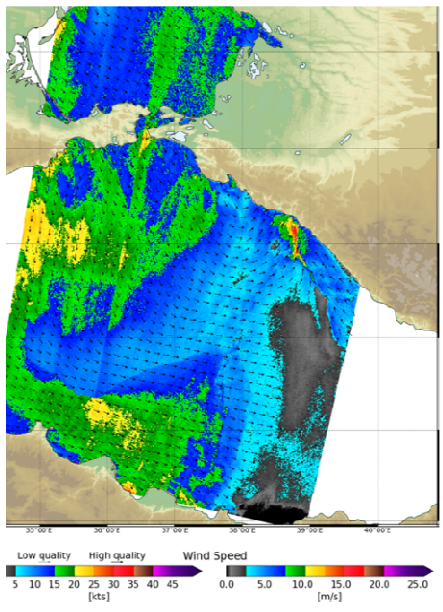

Figure 16. Near-surface wind field derived from the ASAR image depicted in Fig. 11 by including Doppler shift information in the wind retrieval algorithm.

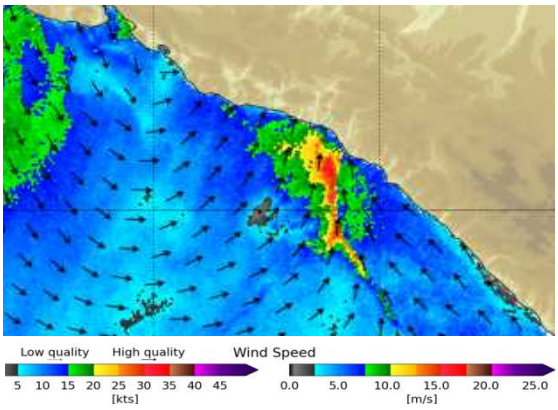

Figure 17. Zoom on the wind tongue visible on the right in Fig. 16 showing that in this area the wind is blowing onto the land and (further south) parallel to the coastline into a northwesterly direction.

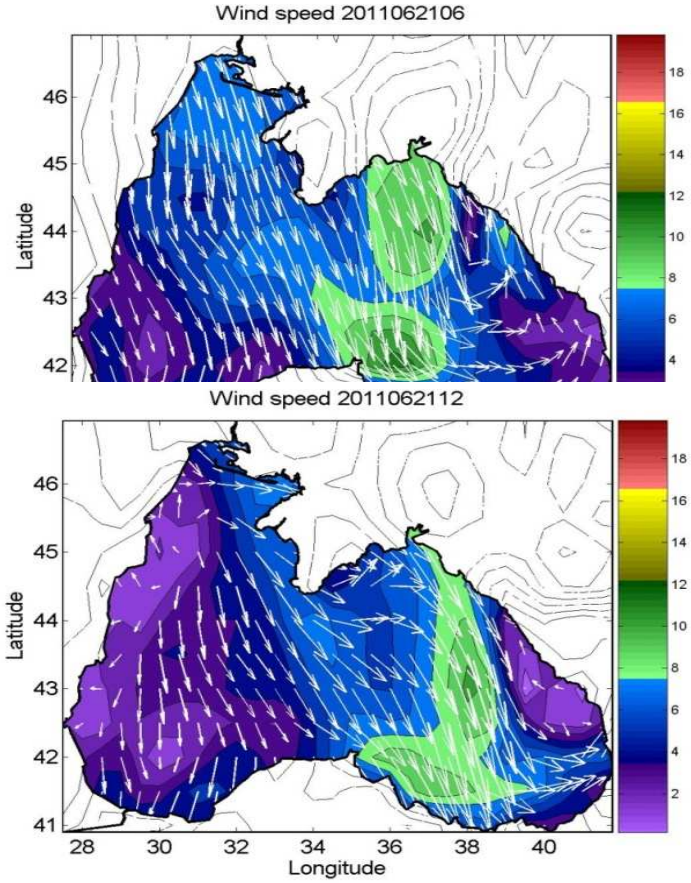

Figure 18. Wind maps of the Black Sea valid for 06 UTC (upper panel) and for 12 UTC (lower panel) on 21 June 2011. The color scale denotes wind speed in m/s. They show a southward directed wind jet emanating from the northern coast. Model resolution: 0.5^0 x 0.5^0. Source: web-site of MHI NASU (Ukraine).

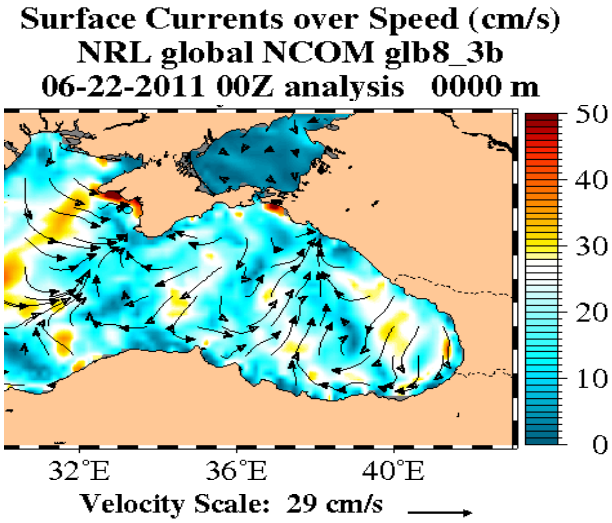

Figure 19. Surface current field calculated from the NCOM model for 00 UTC on 22 June 2011. Note the on-shore current at the northeast coast, approximately at the location of the bright band visible on the ASAR image (Figs. 11 and 12). © MHI NASU

2) The boundary between the two wind fields northwest of coastal mountain range drops abruptly. Thus northeasterly winds can blow onto the sea unimpeded.

The wind field map depicted in Fig. 14, which was obtained from ASAR data using the wind direction from the NCEP model, shows northwest of Tuapse on-shore winds. We tend to explain this mismatch by the coarse resolution of the NCEP model. But also the wind field map retrieved from ASAR data by including Doppler information shows here also on-shore winds (Figs. 16 and 17).

On the other hand, the wind maps of the Marine Hydrophysical Institute in Sevastopol, Ukraine (MHI NASU) (Fig. 18) valid for 06 UTC (upper panel) and for 12 UTC (lower panel) on 21 June 2011, respectively, show southward directed winds emanating from the northern/northeastern coast of the Black Sea. However, on these maps the strong winds emanate from a slightly more northern position at the coast than suggested by the ASAR image.

There are two possible explanations for this mismatch between the wind field maps derived from ASAR data by including Doppler information (Figs. 16 and 17) and the ones provided by the MHI NASU (Fig. 18). First, the contribution of the surface current to the measured Doppler shift has not been taken into account in the wind retrieval algorithm. This supposition is supported by the surface current map depicted in Fig. 19, which is obtained from the US Navy Coastal Ocean Model (NCOM) (available online at: ttp://www7320.nrlssc.navy.mil/global_ncom/glb8_3b/ht

ml/index.html) for 00 UTC on 22 June. It shows an on-shore current northwest of Tuapse.

Second, as observed on Fig. 15, the location, where the discrepancy occurs, corresponds to very low values of the Doppler shift. A Doppler value close to zero means no surface velocity or surface displacement in azimuth direction of the antenna. As a matter of fact, in this example, the inversion led to the second solution, where the wind blows in azimuth direction. Note that an alignment in azimuth direction means a 180° ambiguity in the wind direction (southwesterly or northeasterly wind). However, instead of selecting the wind direction in offshore direction (northeasterly wind), the algorithm picked up the solution where the wind is onshore (southwesterly wind). This wrong inversion is due to the fact that the algorithm combines the information given by the measured Doppler shift and the numerical weather prediction model, which shows onshore winds. Indeed, as shown by Mouche et al., (2012), even when the Doppler shift better constrains the wind inversion, there is still a need for a-priori ancillary wind information (see Fig. 2 of Mouche et al., (2012) [6]). In some cases, like this one, it can lead to imprecise solutions that are a trade-offs between ancillary data and SAR data.

These facts could be the reason for the discrepancy between the SAR-derived wind field and the model wind field of the Marine Hydrophysical Institute.

8. SUMMARY AND CONCLUSIONS

In this paper we have applied a new algorithm developed by Mouche et al. (2012) [6] to retrieve near-surface wind fields over the sea from SAR data acquired by the ASAR onboard the Envisat satellite to three complex wind events over the Black Sea. This algorithm includes, in addition to atmospheric model data and linear features, also Doppler information inherent in the ASAR data for determining both wind speed and direction. It is shown that the new algorithm yields, in general, better wind fields than conventional wind retrieving algorithms. In particular, the strong dependency of the Doppler shift anomaly enables to better constrain the wind inversion in terms of wind direction. However, we have presented one wind event where the new algorithm, when applied blindly, seems not to give a realistic wind field in one specific sea area. We conclude that, even highly promising, the new wind retrieval algorithm still needs some amendments for yielding correct wind fields also in coastal areas with complex coastal topography. Challenging tasks are to properly separate contributions from wind and waves from surface currents and to decrease the weight of the ancillary data in the wind inversion scheme.

ACKNOWLEDGMENTS

We thank ESA for providing the ASAR images free of charge. ESA) and in particular Betlem Rosich who helped modify Envisat ASAR Wide Swath products to include Doppler centroid grids. This work was partly supported by 1) ESRIN/ESA under Contract No. 4000103095/11/I-LG: SAR Ocean Wind-Waves and Current: Upgrade of the Soprano Web Service, and 2) the Russian Government (Grant No.11.G34.31.0078) for research under supervision of the leading scientists at the Russian State Hydrometeorological University.

REFERENCES

1 Alpers, W., Ivanov, A.Yu., & Dagestad, K.-F. (2011). Encounter of foehn wind with an atmospheric eddy over the Black Sea as observed by the synthetic aperture radar onboard Envisat. *Mon. Wea. Rev*., **139**, 3992-4000, doi:10.1175/MWR-D-11-00074.

2 Alpers, W., Wong, W. K., Dagestad, K.-F. & Chan, P. W. (2012). A northerly winter monsoon surge over the South China Sea studied by remote sensing and a numerical model. *Int. J. Rem. Sens*. **33**, 7361-7381.

3 Monaldo, F. M., Thompson , D. R., Beal R. C., Pichel, W. G., & Clemente-Colon, P. (2001). Comparison of SAR derived wind speed with model predictions and ocean buoy measurements. *IEEE Trans. Geosci. Rem. Sens*., **39**, 2587–2600.

4. Horstmann, J. & Koch, W. (2005). Comparison of SAR wind field retrieval algorithms to a numerical model utilizing ENVISAT ASAR data. *IEEE J. Oceanic Eng.*, **30**, 508–515.

5 Sikora, T. D., Young, G. S,, & Winstead, T. S. (2006). A novel approach to marine wind speed assessment using synthetic aperture radar. *Wea. Forecasting*, **21**, 109-115.

6 Mouche, A. A., Collard, F., Chapron, B., Dagestad, K.-F., Guitton, G., Johannessen, J. A., Kerbaol, V., & Hansen, M. W. (2012). On the use of Doppler shift for sea surface wind retrieval from SAR. *IEEE Trans. Geosci. Remote Sen.*, **50**, 2901-2909, doi:10.1109/TGRS.2011.2174998.

7 Stoffelen, A. & Anderson, D. (1997). Scatterometer data interpretation: Estimation and validation of the transfer function CMOD4. *J. Geophys. Res.*, **102** (C3), 5767–5780.

8 Chapron, B., Collard, F., & Ardhuin, F. (2005). Direct measurements of ocean surface velocity from space: Interpretation and validation. *J. Geophys. Res.*, **110**, p. C07008 ASAR surface current velocities *J. Geophys. Res.*, **115**, doi:10.1029/2009JC006050.

9 Rouault, M. J., Mouche, A., Collard, F., Johannessen, J. A., & Chapron, B. (2010). Mapping the Agulhas current from space: An assessment of ASAR surface current velocities. *J. Geophys. Res.*, **115**, doi:10.1029/2009JC006050.

10 Collard, F., Mouche, A., Chapron, B., Danilo, C., & Johannessen, J. A. (2008). Routine high resolution observation of selected major surface currents from space. *Proc. SEASAR 2008 Symp*., ESA SP-656, ESA-ESRIN, Frascati, Italy, 2008.

11 Hansen, M. W., Collard, F., Dagestad, K.-F., Johannessen, J. A., Fabry, P., & Chapron, B. (2011). Retrieval of sea surface range velocities from Envisat ASAR Doppler centroid measurements. *IEEE Trans. Geosci. Remote Sens.*, **49**, 3582–3592, doi:10.1109/TGRS.2011.2153864.

12 Portabella, M., Stoffelen, A., & Johannessen, J. A. (2002). Toward an optimal inversion method for SAR wind retrieval. *J. Geophys. Res.*, **107**, doi:10.1029/2001JC000925.